

# Design, Development, and Testing of Peristaltic Suit: Active Compression and Physiological Sensing Intra-vehicular Activity Spacesuit for Cardiovascular Deconditioning

Irmandy Wicaksono<sup>1\*</sup>, Ali Shtarbanov<sup>2</sup>, Esha V. Ranade<sup>3</sup>, Rebecca Y. Slater<sup>4</sup>,  
Dava Newman<sup>5</sup> and Joseph A. Paradiso<sup>6</sup>  
*MIT Media Lab, Cambridge, MA 02142, United States*

Prolonged exposure to microgravity is known to cause various acute health risks, including muscle atrophy, bone loss, cardiovascular deconditioning, and orthostatic intolerance. Due to the absence of gravitational force, bodily fluid hydrostatic pressure gradients vanish, and blood distribution shifts from the astronaut's legs toward their upper body. Consequently, it is imperative to provide continuous medical check-ups and interventions for astronauts and crewmembers throughout their long-term journey in outer space and also after their return to Earth. This paper presents the design, development, and preliminary parabolic flight testing of Peristaltic (PS) Suit. PS-Suit is an active bioelectronic intra-vehicular activity spacesuit that could simultaneously perform wireless multi-modal monitoring of vital signs, including heart electrical activity, respiration, blood flow, and oxygen level and exert controlled, spatiotemporal and peristaltic pressure through five textile-based compression sensors and five pneumatic chambers integrated across the bodysuit. Integrating physiological and physical sensing and pneumatic actuation systems in the PS-Suit (1) facilitates closed-loop and timely intervention for astronauts to regulate their cardiovascular dynamics and (2) enables researchers to study the direct influence of active-dynamic compression in micro to hypergravity conditions on various cardiovascular and physiological markers. In the end, we tested and evaluated a functional prototype of the PS-Suit during a parabolic flight campaign to investigate the response of heart-rate and blood pulse arrival time to applied gradient compression and changes in gravitational force.

## Nomenclature

ADC	= analog-digital converter	GUI	= graphical user interface
AGS	= anti-gravity suit	HR	= heart rate
BCG	= ballistocardiography	I <sup>2</sup> C	= inter-integrated circuit
BLE	= Bluetooth low energy	I/O	= input/output
BP	= blood pressure	IMU	= inertial measurement unit
BPM	= beat per minute	IR	= infrared
DBP	= diastolic blood pressure	ISS	= international space station
ECG	= electrocardiography	IVA	= intravehicular activity
EVA	= extravehicular activity	LBNP	= low body negative pressure
GCG	= gradient compression garment	LEO	= low earth orbit
GLCS	= gravity loading countermeasure skinsuit	M	= mean (average)

<sup>1</sup> Ph.D. Candidate/Research Assistant, MIT Media Lab, \*[irmandy@mit.edu](mailto:irmandy@mit.edu).

<sup>2</sup> Ph.D. Candidate/Research Assistant, MIT Media Lab.

<sup>3</sup> Undergraduate Researcher, MIT Electrical Engineering and Computer Science.

<sup>4</sup> Undergraduate Researcher, MIT Mechanical Engineering.

<sup>5</sup> Director, MIT Media Lab. Apollo Professor of Astronautics, Harvard + MIT Health, Sciences, and Technology.

<sup>6</sup> Alexander W. Dreyfoos (1954) Professor of Media Arts and Sciences, MIT Media Lab.

OI	=	orthostatic intolerance	SBP	=	systolic blood pressure
PAT	=	pulse arrival time	SMA	=	shape memory alloy
PPG	=	photoplethysmography	SMP	=	shape memory polymer
PTT	=	pulse transit time	SPI	=	serial peripheral interface
PWM	=	pulse-width modulation	SD	=	standard deviation
PWV	=	pulse wave velocity	TPU	=	thermoplastic polyurethane
RR	=	respiration rate			

## I. Introduction

The vastness and mystery of space captivate a whole new frontier for exploration and discovery, offering potential answers to the fundamental questions about the origins of the universe and the limits of human potential. More than six decades have passed since Yuri Gagarin was aboard the Vostok 1 and made history as the first human to travel into space. Extended spaceflight missions, where astronauts live and work at the International Space Station (ISS), have since become a routine, lasting anywhere from three months to a year<sup>1,2</sup>. The ISS serves as a crucial testing ground for the development of technologies and systems necessary for future space exploration missions. It provides a well-resourced infrastructure where scientists and astronauts can conduct research and experiments on the effects of space environments to human physiology and psychology. It is important to note that the space environment is highly extreme and hostile to the human body, as it is characterized by a range of conditions, including an intense solar ultraviolet field, high vacuum, high-velocity micrometeoroid impacts, atomic oxygen erosion, high temperatures, and microgravity<sup>3</sup>. Extra-vehicular activity (EVA) pressurized spacesuits integrated with a life support system can help astronauts to survive the harsh space environment. EVA spacesuits have supported astronauts through spacewalks outside the ISS and explorations in low-earth orbit (LEO) and on lunar missions<sup>4</sup>. While the ISS is designed to protect astronauts from extreme space environments, it cannot shield them from the effects of microgravity, which can have significant impacts to their physiology.

On Earth, humans typically spend about two-thirds of the day upright and about the rest lying down during sleep at night. Upon reaching weightlessness, our body tissues and fluids in the vascular and lymphatic systems are relieved as they become immediately unloaded from their established compressive forces in Earth's gravity. The early crewed space program Gemini (1965) concluded that prolonged microgravity exposure induces various acute health risks, including reduced red cell mass, osteoporosis, skeletal muscle atrophy and fatigue, cardiovascular deconditioning, and orthostatic intolerance<sup>5</sup>. Space programs such as Apollo (1968) and Skylab (1973)<sup>6,7</sup> had also supported long-term research data to further study human physiological adaptations in space and the effectiveness of lower-body negative pressure (LBNP) as a countermeasure technology. Recent research conducted by Marshall-Goebel et al. (2019), through a study that measured the internal jugular vein of 11 healthy astronauts, found that prolonged exposure to microgravity results in a chronic reverse head-ward blood and tissue shift, which could lead to complications such as the formation of blood clots and thrombosis<sup>8</sup>. These findings underline the importance of continuous medical monitoring and intervention for astronauts in long-term microgravity exposure and after their return to Earth. In the context of longer missions, such as a one-way trip to Mars which takes approximately 1.5 years, the significance of ensuring cardiovascular health will become even more critical.

Gravity has a significant influence on bodily fluid hydrostatic pressure gradients. Without it, blood distribution tends to move up towards the upper body. As a countermeasure, astronauts have traditionally used LBNP chambers, orthostatic intolerance (OI) anti-gravity suits (AGS), and gradient compression garments (GCG), which are designed to improve blood circulation and musculoskeletal health, amongst other benefits<sup>9</sup>. However, large countermeasure equipment may not be practical for future spaceflight, owing to its payload and vehicle space requirements<sup>10,11</sup>. On the other hand, a wearable solution such as the GCG cannot adapt to the physical change of the body and maintain constant pressure throughout<sup>12-14</sup>. The tightness of these compression suits also make them hard to put on and off. AGS requires connection to a bulky pneumatic system, which restricts astronauts' mobility<sup>15</sup>. In addition, both GCG and AGS technologies are not responsive and do not dynamically adapt to the physiological changes of the astronauts.

To this end, inspired by the contraction and relaxation of muscles in the human gastrointestinal tract, we have developed Peristaltic Suit (PS-Suit) by embedding an array of soft, textile-based actuators and physical and physiological sensors into a full-body intra-vehicular activity (IVA) suit with miniaturized and wireless sensing-actuation physiological and pneumatic control hardware<sup>16</sup>. Incorporating both sensing and actuation systems enable us to observe the direct influence of active compression on various physiological markers<sup>17</sup>. In summary, our main contributions, which will be covered in this paper, are as follows:

- 1) Description of material and methods of inflatable fabrics for an active compression system in sleeve prototypes
- 2) Design framework and the development process of the full-body PS-Suit
- 3) Implementation of various firmware and hardware elements of PS-Suit, including the physiological and physical sensing system, as well as the pneumatic actuation system
- 4) Skin compression characterization of the active compression system
- 5) Testing the PS-Suit prototype in a parabolic flight to evaluate micro-to-hyper-gravity and gradient compression effects on physiological markers, such as pulse-arrival time (PAT) and heart-rate (HR).

## II. Background and Related Work

### A. Cardiovascular Performance and Monitoring in Space Physiology

The cardiovascular system regulates blood cells, oxygen, nutrients, and waste products around the body, as the blood - its main component - circulates through a closed network of vessels. Blood distribution is heavily influenced by gravity. In an upright position, blood pressure is greater in the feet, which is around 26.7 kPa (200 mmHg) than in the head (~9.3 kPa, 70mmHg), and it is also greater relative to the heart (~13.32 kPa, 100mmHg)<sup>18</sup>. This gradient is lost in space, causing astronauts to suffer from face puffiness and motion sickness within a few minutes of microgravity exposure<sup>19</sup>. Another primary concern impacting astronaut health and safety is landing day orthostatic intolerance. Astronauts with orthostatic intolerance cannot maintain adequate arterial blood pressure and have decreased brain blood levels when upright. Research has found that up to 80% of astronauts experience this condition within four to six hours of landing from long-duration spaceflight<sup>20</sup>. To prevent and reduce the likelihood of orthostatic intolerance, monitoring astronauts' health and performance and providing countermeasures during and after space missions is essential.

Several studies have been conducted to evaluate cardiovascular parameters such as heart rate and blood pressure variability during short microgravity periods in parabolic flights to long-term microgravity in LEO. Aerts *et al.* (2015) concluded that there is a direct relationship between gravity levels to mean systolic and diastolic blood pressure with reduction of blood pressure (BP) responding to lower gravity based on their six participants parabolic flight test with electrocardiogram (ECG), inflatable finger cuff, and photoplethysmogram (PPG)<sup>21</sup>. A study by McCall *et al.* (2015) also conducted a parabolic flight test to study cardiovascular performance in nine participants by using non-invasive measurement of pulse-transit time (PTT), which inversely correlates to systolic (SBP) and diastolic (DBP) blood pressure based on ballistocardiogram (BCG) and PPG signals<sup>22</sup>. They concluded that mean PTT between ground and microgravity for all subjects increased by around 30%. Pulse-arrival time (PAT) between ECG and PPG of the foot has also been used as a non-invasive blood pressure correlation parameter during postural transitions before and after spaceflight, with the results showing cardiovascular deconditioning with heart-rate (HR) increasing by an average of 10/min and SBP/DBP by 0.67/1 kPa (5/8 mmHg) in supine posture after spaceflight<sup>23</sup>. Baevsky *et al.* (2007) conducted a long-term 6-months study, with the addition of one and two months pre-flight and three and six days post-flight on BP adaptation in eight ISS astronauts with an oscillometric monitoring device. The results show that diastolic blood pressure was significantly reduced by 1.33 kPa (10 mmHg) and was stable from beginning to end during the spaceflight, with heart-rate variability unchanged. Three days after spaceflight, both SBP/DBP jumped in average by around 2.67 kPa (20 mmHg), which corresponds to a demand and adaptation in cardiac output<sup>24</sup>.

One of the major limitations of health monitoring in space is that crewmembers are usually tethered to medical equipment, which sometimes can be inefficient and uncomfortable. At the ISS, crewmembers record their vital signs by manually connecting several devices, such as ECG, BP cuff, and vascular sonogram during their daily check-up or exercise routine<sup>25</sup>. With future lunar and Martian missions, it will become increasingly critical for crewmembers to have the capability to monitor and interpret their own health and performance autonomously, so that they can focus on their mission and perform their tasks safely and effectively. Astronauts will require non-invasive and remote diagnostic systems with decision-support features based on their real-time physiological data. In this light, wearable technologies, electronic textiles, and smart clothing developed for personal health, physical activity, and safety applications on the Earth can be adapted for space applications<sup>26-31</sup>. Astroskin, a smart shirt initially launched with SpaceX CRS-16 in 2018, for example, can measure multitude physiological parameters such as blood pressure, electrophysiology, breathing rate, temperature and blood oxygen level<sup>32,33</sup>. The continuous advances of these technologies have shown the potential in developing and integrating new sensing modalities and actuation systems for personalized telemedicine and seamless medical intervention in outer space<sup>34-36</sup>.

## B. Countermeasure Technologies and Compression Suits

In the last decades, new solutions to mitigate the cardiovascular and musculoskeletal effects of microgravity have been implemented in the ISS. Crewmembers are required to exercise for at least two hours per day using equipment such as bicycle ergometer, treadmill, bungee cord, an elastomer providing a resistance exercise, and the Advanced/Interim Resistive Exercise Devices<sup>10,37</sup>. Another solution is to simulate gravity itself. The best way to achieve this is to exploit the centripetal force produced by a centrifuge. However, building a centrifuge on a sufficient scale is challenging for space missions with constrained budgets and space<sup>9</sup>.

As shown in Figure 1, several wearable countermeasures have been designed and tested for spaceflight, including the Chibis suit, Pingvin suit, the Skylab Cardiovascular Counter Pressure Garment, the Shuttle AGS, the Kentavr, and the more recent GCG and the gravity-loading countermeasure skinsuit (GLCS). The lower body negative pressure (LBNP) chamber or commonly known as Chibis suit (Figure 1a) provides an effective cardiovascular countermeasure by pulling fluid down to the legs in a vacuum chamber and expanding veins and tissues of the lower body<sup>7</sup>. This system immobilizes astronauts as they need to submerge their body hip down into a chamber. The Pingvin suit (Figure 1b) uses bungee cords to provide longitudinal compression and resistance against normal posture to encourage muscle activation<sup>13</sup>. It has elastic bands connected to a waistband that create tension between the waist and the feet and between the shoulders and the waist with reported 50% of bodyweight loading. The design, however, only allows two discrete loading levels, making it uncomfortable and thermally unviable if worn for the recommended 8 hours, often hindering activity and exercise performance<sup>9</sup>. The GLCS (Figure 1g) employed a bi-directional elastic weave and is customized to the wearer for comfort and a higher and more distributed loading resolution<sup>14,38</sup>. Both the Pingvin suit and GLCS are geared toward reducing effects such as bone deterioration, muscle atrophy, and spinal elongation.



**Fig.1: Various IVA wearable countermeasure technologies, including a) Chibis Suit<sup>45</sup>, b) Pingvin suit<sup>46</sup>, c) Skylab Cardiovascular Counter Pressure Garment<sup>39</sup>, d) Shuttle Anti-gravity Suit<sup>47</sup>, e) the Kentavr<sup>48</sup>, f) Gradient Compression Garment<sup>40</sup>, and g) Mk-7 Gravity-Loading Countermeasure Skinsuit<sup>38</sup>.**

For orthostatic intolerance and cardiovascular deconditioning wearable countermeasures, the Skylab Cardiovascular Counter Pressure Garment (Figure 1c) employed inflatable tubes that can be pressurized manually through a single bulb<sup>39</sup>. The mechanism was applied in partial pressure suits for pilots and jet fighters for many years prior to the development of fully pressurized suits. Upon inflation, the tubes expand and tighten the circumference of the leg, applying pressure mechanically. The garment was patterned such that the applied pressure was greatest at the ankles, and progressively less pressure was applied to the top of the thigh. The Shuttle AGS (Figure 1d), a more advanced example, is a pneumatic partial pressure system comprising five interconnected pressure bladders that covers the lower abdomen to the ankle<sup>15</sup>. Adapted from its use for military and jet pilots in the 80s, the AGS is an active garment that can be controlled through a pneumatic system and inflated to give pressure in the range of 3.59 to 17.2 kPa (26.9 to 129.3 mmHg). The primary disadvantage of AGS is that it requires the wearer to be stationary. It is not optimized for wearability and mobility, as the air pipe is wired to a bulky pneumatic system. The pressure in the inflatables used as an actuator also does not represent the actual pressure exerted on the body, making it less effective as a compression suit.

The Kentavr (Figure 1e) and the recent GCG (Figure 1f), on the other hand, are made of a passive elastic fabric with the form-factor of a pant and a suspender overall, respectively. The Kentavr is adjusted using lacing panels on each component, allowing for a customizable fit to each subject and providing approximately 4 kPa (30 mmHg) of compression<sup>15,40</sup>. The GCG is tailored to the individual from the lower abdomen to the foot and is designed to produce a fixed gradient compression force of 2.1 kPa (16 mmHg) in the abdominal region to 7.33 kPa (55 mmHg) around the

ankle<sup>41</sup>. However, compression garments are difficult to don/doff and are not able to exert dynamic or controllable pressure on the body. They also do not adapt to the physiological and physical changes of the astronauts. Several efforts have explored smart materials such as shape memory alloy (SMA) to develop morphing or dynamic compression garments, with BioSuit, a skintight mechanical counterpressure spacesuit that could substitute for modern gas-pressurized suits, as an example<sup>42-44</sup>. SMA integration and application into spacesuits are still under research, as they are relatively stiff for IVA garments and spacewear and require high current or temperature actuation. Consequently, there is a need for a smart compression garment that offers dynamic and spatiotemporal controls based on the physical and physiological changes of the astronauts. This smart garment must also incorporate wearable and lightweight systems designed for IVA during long-term space travel.

### III. Active Compression System Design and Development

#### A. Materials and Methods

Pneumatic compression devices have been widely used for aiding the circulation of blood and lymphatic fluid in sports, rehabilitation, and medical settings. Pneumatic controls and inflatable pouches were leveraged for the actuation hardware (Section IV), as they afford the system requirements. To develop active compression components based on soft textile-based pneumatic actuators, thermoplastic polyurethane (TPU) film, as typically implemented in hot-melt adhesives (e.g., HM65, Perfectex), were used. An inflatable bladder was fabricated by thermally-welding two layers of TPU film with an impulse sealer (FS400, Fuxury). A hole was then punctured for the pneumatic tubing opening (1.5mm, uxcell) and sealed with soft silicone rubber glue (RTV 732, Dow Corning). A two-terminal textile pressure sensor for quantifying the compression force was developed by sandwiching a piezoresistive knit fabric (LTT-SLPA-60k, Eeonyx) in between two conductive knit fabrics (Stretch Conductive Fabric, Less EMF) and connecting TPU-insulated conductive threads (117/17 dtex silver-coated nylon, Statex). The textile pressure sensor leverages the piezoresistive effect, in which a force exerted onto a functional fabric compresses its percolated conducting structure, forming more electrical network, and thus, reduces its resistance<sup>49,50</sup>.

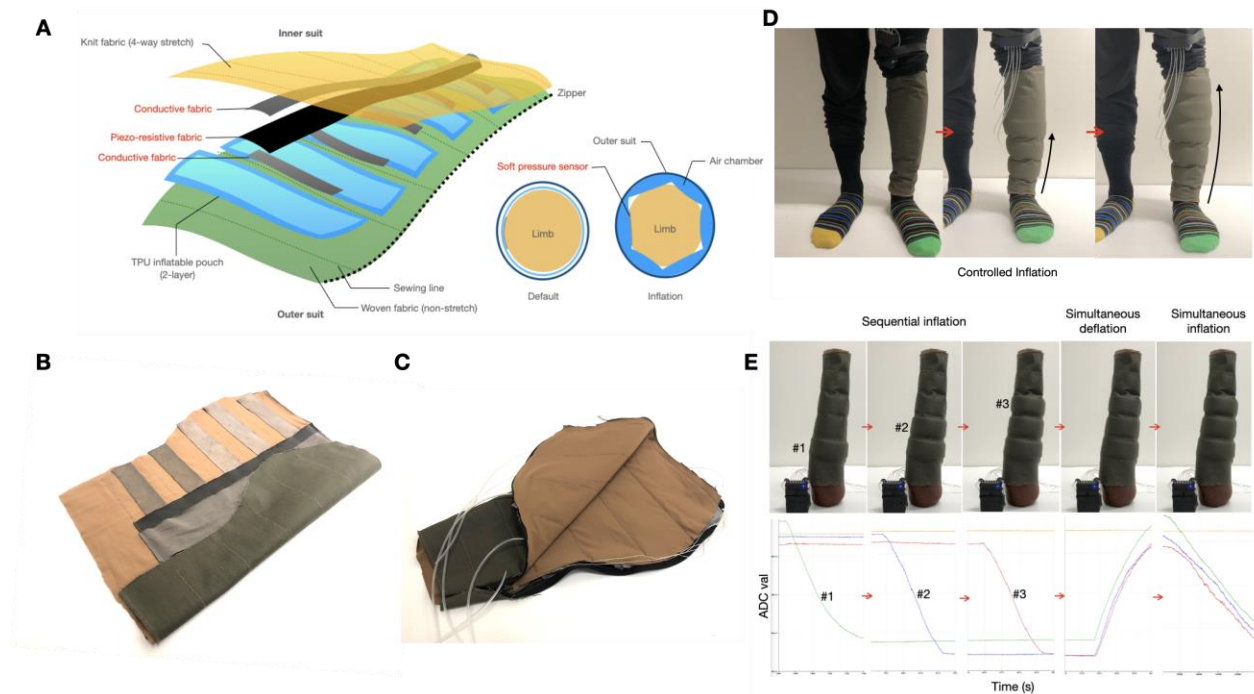


**Fig.2:** a) Exploded view and illustration of an active compression sleeve prototype, b) Internal textile pressure-sensing array layer and c) final prototype of a calf sleeve integrated with air tubing. d) Demonstration of a peristalsis dynamic compression movement from ankle to knee. E) Arm sleeve prototype actuated sequentially and simultaneously with real-time compression pressure sensing.

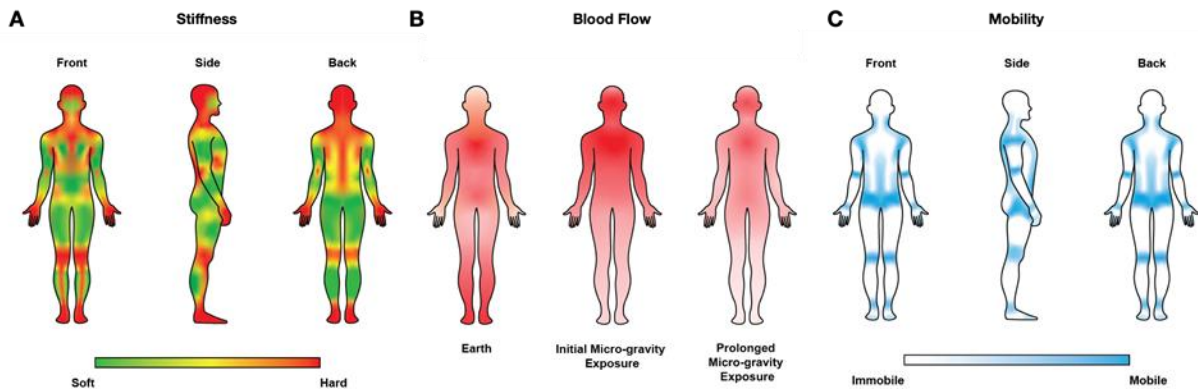
## B. Implementation

Figure 2a illustrates a design of an active compression sleeve with an array of five fabric bladders. An outer woven fabric and an inner 4-way stretch fabric are patterned with openings in which to embed the inflatable pouches. The mechanical properties of these fabrics restrict and provide positive compression force toward the limb as the inner bladders are inflated. Free-standing TPU bladders were integrated inside a textile sleeve, instead of fused onto a textile with a heat press machine. This technique made it easy to replace the bladder in the case of a damage or puncture. A two-terminal textile pressure sensor (with a shared ground) for quantifying the compression force is developed by sandwiching a piezoresistive knit fabric (LTT-SLPA-60k, Eeonyx) in between two conductive knit fabrics (Stretch Conductive Fabric, Less EMF) with an active force-sensitive area of 3 x 3 cm and connecting TPU-insulated conductive threads (117/17 dtex silver-coated nylon, Statex).

Active compression calf (Figure 2b-c) and arm (Figure 2e) sleeves were developed by embedding five inflatable pouches into a customized textile structure and connecting it to FlowIO, our miniaturized pneumatic system<sup>51</sup>. As shown in Figure 2d, controlled compression and sequential inflation on each chamber can be applied to mimic the peristaltic movement. Figure 1e shows the compression pressure data of each chamber as the active compression arm sleeve is inflated and deflated sequentially or simultaneously. A force exerted on each fabric pressure sensor reduces its resistance, which is shown as a drop in the analog-digital converter (ADC) value.

## IV. The Peristaltic Suit System

When it comes to garments worn during various activities, ergonomic comfort is crucial, particularly for activewear and protective clothing like spacesuits. The mechanical characteristics of spacewear should align with the degree of freedom, range of motion, force, and moment of human joints. The garment's shape and fit relative to the human body and the pressure it exerts on the body significantly affect its ergonomic properties. Therefore, the design of compression spacesuits must balance the application of sufficient body surface pressure while enabling free movement, necessitating a comprehensive understanding of the biomechanics of human tissue and the cardiovascular system. Figure 3 shows illustrations of a human body stiffness map based on muscular and bone tissue distribution<sup>52</sup>, a blood distribution map due to microgravity exposure<sup>53</sup>, and a mobility map based on body joints<sup>54</sup> that inform our IVA spacesuit design.



**Fig.3: Qualitative mapping of the human body a) average tissue modulus, b) blood flow distribution during initial and prolonged microgravity exposure, and c) active and passive mobility areas.**

### A. Suit Design

From blood flow mapping, it is known that microgravity exposure in space leads to the redistribution of fluids in the body, causing a shift of fluids toward the upper body and away from the lower limbs. This shift can lead to a decrease in blood volume and cardiac output, which, over time, can lead to cardiovascular deconditioning. In addition, orthostatic intolerance refers to the body's inability to remain upright and maintain normal blood pressure and blood flow to the brain and throughout the body. To address these conditions, spatiotemporal gradient compression that could help regulate blood flow and pressure, and function similarly to GCG and Chibis suits, should be integrated into a full-body spacesuit<sup>7,40</sup>. In this case, IVA spacesuit design was considered, since astronauts spend most of their time conducting scientific experiments and performing essential daily tasks inside a space station.

The morphology and heterogeneous tissue properties of the human body influence the evenness of skin pressure exerted by a compression suit<sup>52,55</sup>. If the compression is not applied correctly, it can cause discomfort, restrict movement, and even lead to injury. The anterior tibia region, for example, absorbs and dissipates compression less than the posterior elastic muscular region, since it has a higher stiffness due to the bone tissue density. Therefore, the compression suit must be personalized to the wearer's body. The pneumatic, inflatable chambers should also be effectively distributed around the soft muscle regions to maximize pressure delivery throughout the body and regulate blood flow, while avoiding areas where they disrupt mobility, such as the body joints<sup>53,54</sup>. The conformability of the suit is also important to achieve robust sensor-skin contact for long-term continuous physiological sensing<sup>26</sup>.

To acquire precise measurements of the wearer, a Lenscloud 3D photogrammetry system comprising 120 cameras was operated to produce 360° scans of body contours (Figure 4a). The images, stored in RealityCapture, are then processed to generate the 3D model (Figure 4b) and transferred to a 3D modeling software (Blender). By transforming the 3D model into a field of vertices, marking the seam, and then unwrapping it, a 3D model of the human body can be converted into a collection of garment patterns. These user-centric garment patterns can also be transported into a 3D garment or clothing modeling software (Clo3D, Figure 4c) in order to visualize the fit. Figure 4d and 5a present the vision of the PS-Suit with inflatables or pneumatic chambers fully-distributed across the body. The current version of the pneumatic system (the FlowIO Platform) limits the PS-Suit to having five inflation and vacuum controls (Figure 4e), although other FlowIO modules can be integrated to incorporate more channels and cover other body parts.

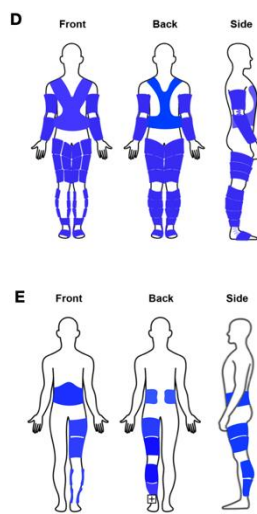
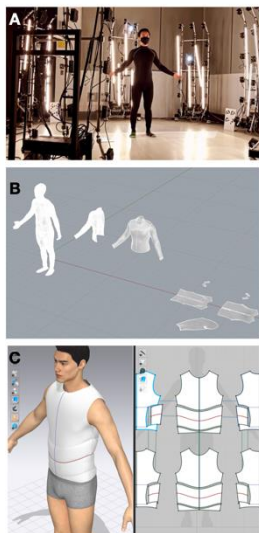


**Fig.4:** a) A subject in a Lenscloud 3D photogrammetry system, b) Garment pattern results after 3D modeling and unwrapping and c) visualization in Clo3D, d) Conceptual and e) actual inflation chambers placement.



**Fig.5:** a) PS-Suit concept and b) illustration of our recent prototype flown in a parabolic flight, showing all the main component of the system (inflatable chambers, fabric compression sensors, physiological sensors, and main wireless module).

For long-duration space flights, the durability of IVA clothing is also crucial. The garment's fabric needs to be strong and tough enough to endure wear and tear. In addition to durability, safety is also a crucial consideration in designing IVA clothing. While protection from extreme external environments is not necessary, safety concerns for indoor clothing still exist<sup>56</sup>. For instance, fire protection is a significant issue in oxygen-rich environments. The PS-Suit's outer layer is adapted from a high-performance Nomex racing suit (Profox) with a combination of knitted Nomex around the joints for freedom of movement and a double-layer quilt-woven Nomex throughout. Nomex is a high-performance fiber with excellent temperature and mechanical resistance and can be found as a base material complementing Gore-Tex and Kevlar in Ortho-Fabric, the outermost layer of EVA spacesuits<sup>57</sup>. The seams of the racing suit were cut and tailored based on the wearer's body circumferences that were measured through the 3D photogrammetry and modeling. The materials of the fabric with the forms of the suit ensure the overall protective and compression functionality, mobility, and comfortability of the PS-Suit for IVA.

The working prototype of the PS-Suit, as shown in Figure 5b and Figure 6d-f, consists of an array of inflatable chambers (five chambers distributed from the lower abdomen to the ankle) in one leg with a physiological and physical

activity sensing system and a pneumatic actuation system that enable both multimodal physiological sensing and active-dynamic compression. The inflatable chambers were integrated by sewing inner 4-way stretch fabrics and embedding free-standing TPU bladders and piezoresistive-based textile pressure sensors, as discussed in detail in Section III.

## B. Physiological and Physical Sensing System

The physiological and activity sensing module (Figure 6a) comprises a set of skin-contact physiological sensors embedded in multiple locations across the PS-Suit (MAX30105 from Maxim and ADS1292R from Texas Instruments) and connected to their central processing system with Bluetooth low-energy capability (BLE, Feather NRF52840) through inter-integrated circuit (I<sup>2</sup>C) and serial peripheral interface (SPI) lines. It includes three biopotential and bioimpedance electrodes around the upper left chest (LC), right chest (RC), and lower left (LL) region of the body to monitor the heart's electrical activity or electrocardiography (ECG) and respiration. The respiration sensing is done through impedance measurement from these electrodes using an ADS1292R (Analog Devices)<sup>58</sup>. LC, RC, and LL cables were integrated from our main module into three different locations in the upper-body region of the PS-Suit with snap connections for attaching the adhesive electrode pads.

Two blood-flow sensing nodes are also distributed around the left toe and right toe through the wearer's shoes. Our blood flow sensing mechanism is based on photoplethysmography (PPG), in which a light-emitting diode (red, infrared/IR, and green) illuminates the skin and a photodiode captures the reflected signal and light absorption caused by the blood circulation<sup>59</sup>. Blood oxygen saturation level can be derived from PPG based on the ratio of red vs IR light absorbance. Furthermore, by processing the ECG and PPG data, we can infer a pulse arrival time (PAT) that correlates to the wearer's pulse wave velocity and blood pressure without needing an inflation cuff that could interfere with the circulation<sup>22</sup> (in principle, as the suit is composed of inflatable elements, a cuff can also be intrinsically implemented if warranted).

Five piezoresistive textile-based compression sensors distributed around the body and lower-leg are read through the ADC inputs of the system. An inertial measurement unit (IMU) for gravity/tilt/acceleration data analysis and physical activity sensing is also integrated in this module. A graphical user interface (GUI) has been developed to visualize all the compression, physical activity, and physiological sensor data continuously in real-time (Figure 6b,7b). In summary, with our system and existing algorithms, the PS-Suit can perform wireless multimodal physiological and compression monitoring including,

- 1) Heart rate and electrical activity of the heart through ECG signal
- 2) Breathing rate and volume through ECG impedance sensing
- 3) Blood flow and pulse-rate through the PPG signals
- 4) Blood oxygen saturation through the PPG signals
- 5) Skin temperature through the on-board pulse-oximetry temperature sensors
- 6) Pulse-arrival time on each leg/toe through peak time-difference between ECG and PPG signals
- 7) Physical activity and gravity levels through the IMU data
- 8) Five compression forces distributed throughout the PS-Suit

For the parabolic flight testing and evaluation, since the focus of the experiment was on dynamic compression and cardiovascular physiological sensing, we activated and recorded only a subset of these parameters: ECG, two PPGs, acceleration, and five compression sensors. Overall, the physiological and physical sensing system operated at approximately 100 Hz including the BLE wireless data transfer operations.

## C. Pneumatic Actuation System

The FlowIO pneumatic system (Figure 7a,c) consists of miniature motor pumps, circuits, and valves that can be wirelessly controlled through BLE and a microcontroller (Feather nrf52840) to control a set of five air chambers distributed throughout the PS-Suit. The entire system is designed to be compact and light-weight, especially for wearable applications<sup>51</sup>. In our case, the pneumatic system with the physiological and physical sensing system are both stored in the pouch on the right side of PS-Suit and attached with a strap (Figure 6c). The main module of FlowIO contains 7 normally-closed solenoid valves in a manifold configuration, of which two are for inlet and outlet (Figure 7b), and the remaining 5 valves for programmable pneumatic input-output (I/O) ports with each port supporting the following functions:

- 1) Inflation
- 2) Vacuum
- 3) Release to atmospheric pressure
- 4) Pressure hold



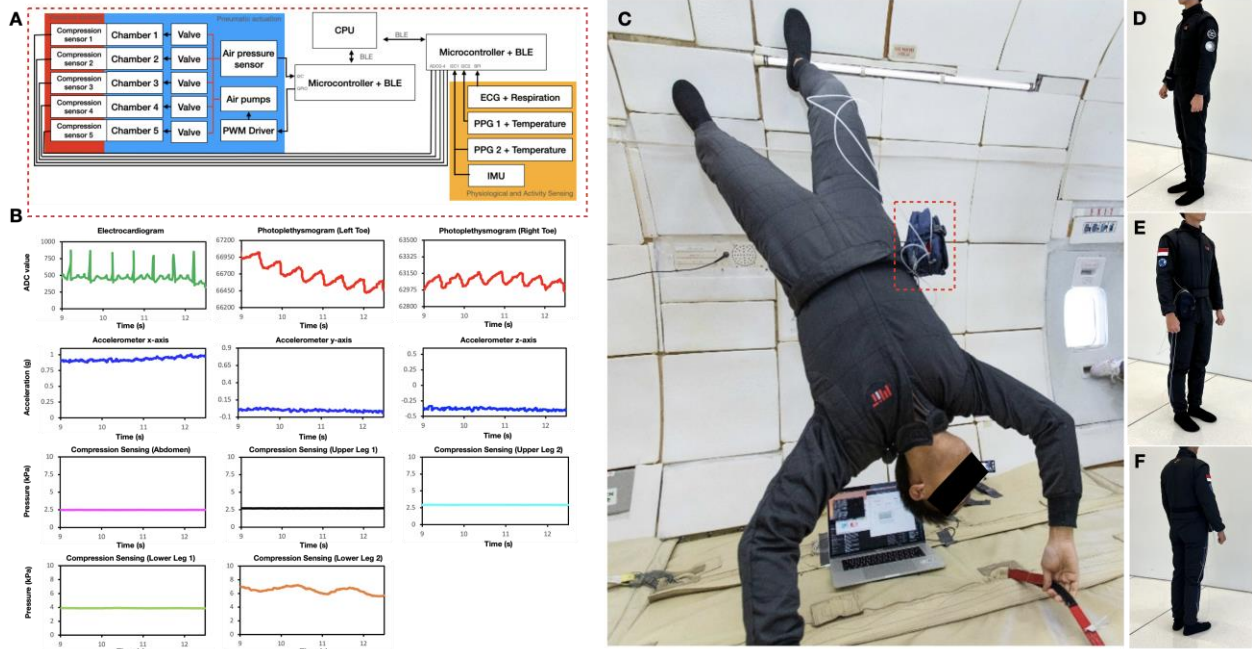


**Fig.6: a) System schematic of the physiological and activity sensing module and pneumatic actuation module, b) wireless real-time recording of all sensing units, including physiological sensors (ECG and PPG on both toes), accelerometers, and compression sensors (indicating a pressure gradient), c) a test subject wearing tailored PS-Suit in a parabolic flight, and d-f) the final prototype of PS-Suit captured from various angles.**

- 5) Pressure sensing
- 6) Flow-rate variability

The same pneumatic action can also be performed simultaneously on more than one port. The choice of normally-closed valves allows pressure hold to occur by default, and therefore the system can maintain different pressures at different ports, even in the off-state. While inflation and vacuum rely on the pumps, pressure release is passive and can happen from an initial state of either high pressure or vacuum. The pressure release operation exploits the fact that the pumps allow one-way flow even when not powered. Finally, flow rate variability is achieved by driving the pumps with pulse-width modulation (PWM) signals at variable duty cycles. Inflation chambers in the PS-Suit can be actuated subsequently to reach a certain compression pressure value, for example, and then they can all be deflated simultaneously by opening all the pneumatic I/O ports. In the case of intense physical activity or a sudden change in atmospheric pressure that would exert high pressure on the inflated chambers, pressure release can be set so that the inflation chambers can adapt and avoid bursting by releasing air passively.

Besides the standard configuration used here, our system supports 4 additional configurations, where the pumps can be connected in series or in parallel, and used either for inflation or for vacuum (Figure 7b). A series configuration achieves higher pressures, while a parallel configuration achieves higher flow rate. If inflation and release capabilities are required instead of vacuum, an inflation series or parallel configuration can be implemented to maximize performance. On another hand, if only vacuum and release capabilities are required, the tubing can be reorganized for vacuum series or parallel configuration instead. We used a Li-Po battery with a high C-rate (45C and 7.4V, AWANFI) to run 3V direct current (DC) air pump (RK-528TB, Skoocom) that can provide flow rates of up to 4.5L/min and a pressure range of -60 to 150kPa (Figure 7d,e).

## V. Evaluation and Discussion

A parabolic flight study was conducted to test the functionality of the PS-Suit for wireless physiological sensing and dynamic compression in extreme gravity environments. It involved a series of rapid ascents and descents, creating periods of zeroG and hypergravity that simulate the environments astronauts experience during space missions. This preliminary study was run to provide insight into any necessary adjustments needed by our spacesuit design and

operations to ensure that the system can withstand the rigors of spaceflight and the ISS environment expected during further development and testing.

All experiments were conducted in compliance with the guidelines of an IRB and were reviewed and approved by the ZERO-G Corporation and the Massachusetts Institute of Technology Committee on the Use of Humans as Experimental Subject (COUHES Protocol 2102000313). A male volunteer with no prior medical history of chronic cardiovascular or skin problems, mental health disease, or physical disability was recruited for participation in this test. Signed consent, including consent of photography during the test, was obtained from the individual after passing the pre-screening procedure. The subject wore the PS-Suit during cruising before the first set of flight parabolas, lay-

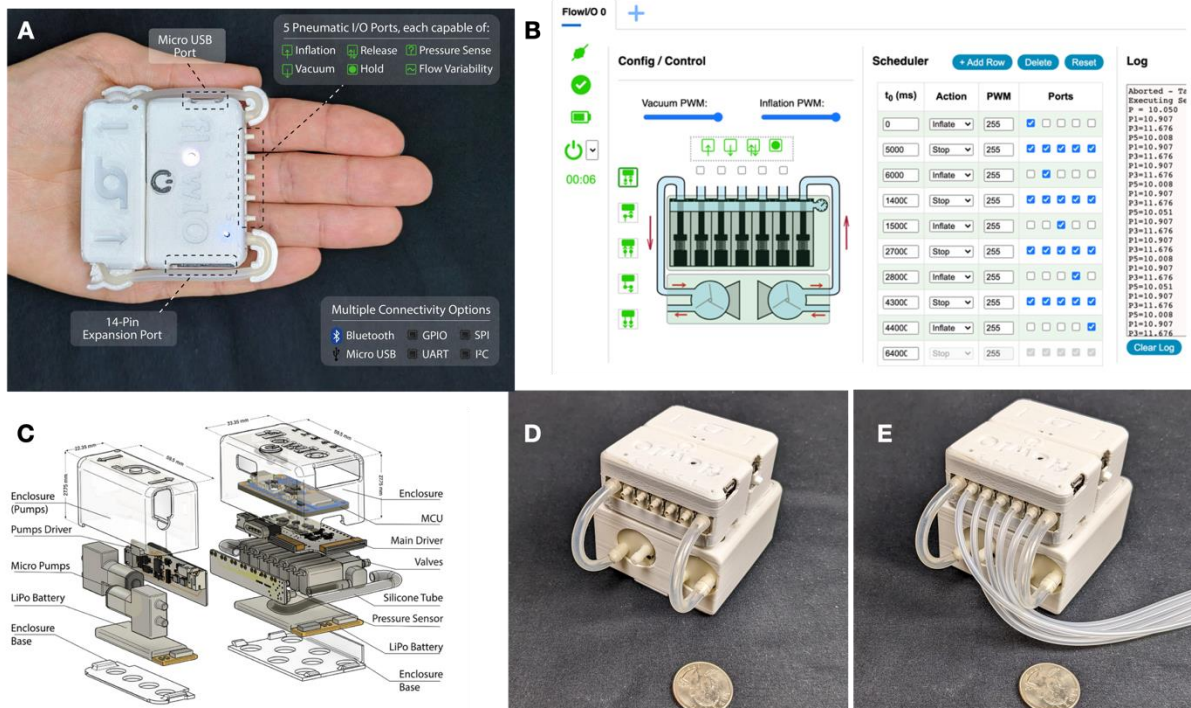


**Fig.7: a) FlowIO pneumatic system that controls all the inflatable chambers for peristaltic pressure and gradient compression in the PS-Suit, b) GUI for controlling the five air flow valves, flow-rates, and scheduling the time of inflation and vacuum/deflation, c) exploded views of all the components making up the pneumatic system, d) pocket-size, light-weight system (coin for comparison) with e) each output valve connecting to the corresponding inflatable chamber through air tubes.**

down on the floor during the hyper-gravity periods, and oriented in head-down positions during the microgravity periods. In the case of emergency, overcompression, or discomfort, a switch can be activated to quickly vacuum all of the air chambers in the PS-Suit. In addition, zippers distributed across the suit can also be used to immediately take it off.

During the parabolas, the PS-Suit’s main module captured and sent data (100 Hz) from an ECG, two PPGs in RL (right leg) and LL (left leg), acceleration ( $x$ ,  $y$ , and  $z$ -axis), and five fabric compression sensors to a computer through BLE communication for logging (Figure 6b,c). The main module also controlled the pneumatic system and five air chambers from the computer through BLE communication (Figure 6b) to provide waist-high gradient compression. The first set of parabolas was used for acclimatization and experiment preparation (making sure that the PS-Suit system and data transfer were all functioning properly), the second set for pneumatic system activation to simulate gradient compression, and the third and fourth sets for physiological adaptation monitoring and evaluation as the gradient compression was constantly applied on the RL until the end of the parabolic flight study.

### A. Compression Characterization

To find the relationship between the fabric resistive compression pressure’s output in  $\Omega$  with skin compression value in mmHg, a ground-test study was also conducted. A high-accuracy sub-bandage pressure monitor was used

(Kikuhime, TT Meditrade) for cross-validation purposes. As illustrated in Figure 8a, compression pressure in mmHg rises as the inflation time increases, and it is inversely proportional to the pressure sensor's resistance. Based on the real-time ADC values of every inflatable pressure sensor during our parabolic flight campaign in Figure 6b-c ( $ADC_{val}$  in succession: 650, 625, 600, 475, and 225) that correspond to inflation time, the effective skin compression pressure can be determined by first calculating the compression resistance from Equation 1 and 2.

$$\frac{R_{ref}}{R_{ref} + R_{compression}} \times V_s = \frac{ADC_{val}}{2^{ADC(bits)}} \times V_{ADC(ref)} \quad (1)$$

$$R_{compression} = \frac{R_{ref} \times ADC_{val}}{2^{ADC(bits)} - ADC_{val}} \quad (2)$$

With  $V_s = V_{ADC(ref)} = 3.3 V$ ,  $R_{ref} = 6.8k \Omega$ , and  $ADC(bits) = 12$ ,  $R_{compression(1-5)}$  can be calculated and then fit to a smooth curve as shown in Figure 8b. From the figure fitting, an applied gradient compression in the PS-Suit of around 2.4 kPa (18 mmHg) in the lower abdomen, 2.6 kPa (21 mmHg) in the upper leg regions, 3.9 kPa (30 mmHg) around the lower leg, and 7 kPa (52 mmHg) closer to the ankle was observed. These compression values (Figure 8c) satisfied the typical compression requirement for countermeasure support against spaceflight orthostatic intolerance during re-entry, landing, and post-landing<sup>39</sup>. Not only can it achieve a compression gradient typical for an OI and GCG suit<sup>40,41</sup>, the PS-Suit can also exert a compression level higher than that typically used for medical purposes (Class 4).

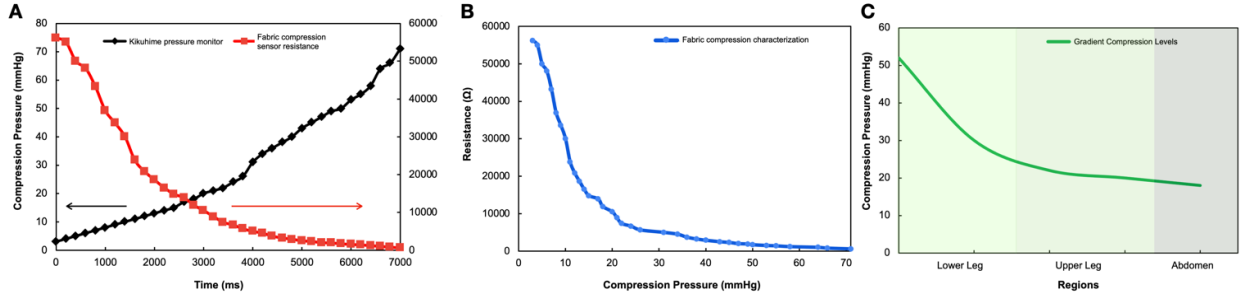


**Fig.8: The relationship between a) actuation time of an embedded bladder (~15 x 20 cm) and compression pressure with Kikuhime pressure monitor (mmHg) and the integrated piezoresistive sensor ( $\Omega$ ), b) resistance of the piezoresistive sensor vs compression pressure, and c) compression pressure level vs body region. Fig.8: The relationship between a) actuation time of an embedded bladder (~15 x 20 cm) and compression pressure with Kikuhime pressure monitor (mmHg) and the integrated piezoresistive sensor ( $\Omega$ ), b) resistance of the piezoresistive sensor vs compression pressure, and c) compression pressure level vs body region.**

## B. Physiological Adaptation during Parabolic Flight

Heart-rate variability and blood flow can give us insights into the modulation of the cardiovascular system. One of the purposes of PS-Suit testing on the third and fourth of the parabolic flight is to measure and analyze the change in these physiological parameters throughout various gravity levels: normal, hyper, and microgravity and under waist-high gradient compression. As shown in Figure 9a, there were a total of 20 parabolas separated into four sets with a few-minute break (~1 g) in between. The first set consisted of two cycles of lunar gravity (~0.16 g), two cycles of Martian gravity (~0.38 g), and a cycle of microgravity (~0 g), each running for around 20 s with approximately 20 s of hypergravity periods in between (~1.8 g). The rest of parabolic flight sets constituted five 20 s cycles of microgravity (~0 g) and hypergravity (~1.8 g) periods (Figure 9c).

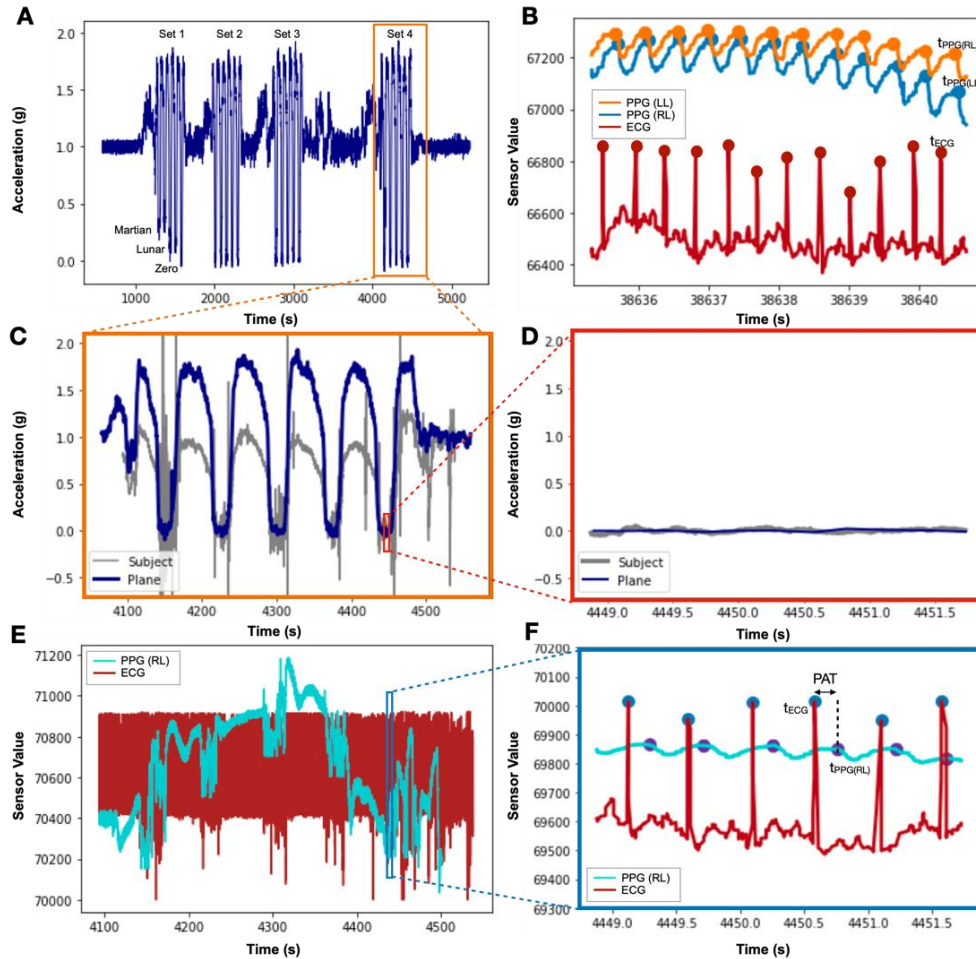


**Fig.9:** a) G-force of the parabolic flight measured through an IMU bolted to a frame on the surface of the plane, b) An example of ECG and PPG data of the parabolic flight test subject for peak-to-peak PAT finding, c) IMU acceleration data of the plane and of the subject showing zero and hypergravity periods during the fourth parabola set with d) zoomed-in microgravity acceleration, e) Right-leg PPG and ECG data during the fourth parabola set with f) a zoomed-in version showing the sequence of peaks in both signals.

Current BP measurement devices employ an inflatable cuff and mechanism and thus cannot be used for rapid and continuous measurement of cardiovascular dynamics. One of the primary cuffless, unobtrusive approaches used to gauge blood flow is through measuring PTT using on-skin or on-body PPG sensors, which indicates the time difference between two pulses at two different locations (two PPG signals), or the PAT, which is the time it takes for a pulse to travel from the heart (defined by a peak in ECG signal or the R-wave) to a peripheral artery (measured by PPG on finger, ear, or toe, for instance). PAT and PTT have been found to indicate changes in pulse wave velocity and are inversely correlated to systolic blood pressure<sup>22,23</sup>. Since the cardiovascular track is the longest from the heart to the toe, and we are applying compression from the body to the ankle with the PS-Suit, we are interested in measuring the PAT through our ECG electrodes on the chest and PPG sensor that we embedded on the shoe to interface with each toe. A previous study discovered that PAT on the toe showed a superior performance as an SBP indicator than PAT and PTT measurement on the fingers<sup>60</sup>.

In order to calculate the length of this PAT interval, the time of all ECG and PPG waveform peaks must be found. This involves a peak-finding algorithm, composed of a noise-reducing process, an algorithm to identify where the curve changes from increasing to decreasing, and a filter to remove fluctuations that do not truly constitute peaks from the final set of peaks returned. This peak-finding algorithm was performed independently on both the raw ECG and PPG data. The noise-reducing algorithm involves averaging the five nearest data points in order to observe the general trends of the curves rather than being sensitive to every fluctuation in the data. The next step computed the differences

between consecutive data points in the averaged data and determined whether the sign of this difference changed since the previous calculation. If the difference changed from positive to negative, it means that the curve's behavior is changing from increasing to decreasing, indicating that a peak has occurred. The detected PPG<sub>peak</sub> should be at a convex maximum of the pulse wave. Figure 9b shows a sample of ECG and PPG data on the left-leg (LL) and right-leg (RL), with each peak represented as  $t_{\text{ECG}(R\text{-peak})}$ ,  $t_{\text{PPG}(LL)}$ , and  $t_{\text{PPG}(RL)}$ . Our algorithm criteria are that the detected PPG<sub>peak</sub> should exist right after an ECG<sub>R-peak</sub> and before the next one (Equation 3).

$$t_{\text{ECG}(R\text{peak})}(n) < t_{\text{PPG}(LL)}(n), t_{\text{PPG}(RL)}(n) < t_{\text{ECG}(R\text{peak})}(n+1) \quad (3)$$

$$\text{PAT}_{(LL)}(n) = t_{\text{PPG}(LL)}(n) - t_{\text{ECG}(R\text{-peak})}(n) \quad (4)$$

$$\text{PAT}_{(RL)}(n) = t_{\text{PPG}(RL)}(n) - t_{\text{ECG}(R\text{-peak})}(n) \quad (5)$$

$$\text{BPM} = \frac{60}{\Delta t} \quad (6)$$

$$\overline{\Delta t} = \frac{n}{\sum_2^n (t_i - t_{i-1})} \quad (7)$$

Once the peaks of the heart rate and pulse waves are identified, the next step is computing the delay between them. A specific PPG peak corresponds to the ECG peak that it follows, and the difference is taken between the timestamps of both peaks. These values are averaged to find the approximate PAT for a given time interval (Equation 4 and 5). The same peak-finding algorithm is used to calculate the Beats Per Minute (BPM) or HRV from an ECG signal. By finding the average time ( $\overline{\Delta t}$ ) between consecutive numbers of peaks ( $n$ ) and dividing 60 by this value, the average number of heartbeats per minute can be determined (Equation 6 and 7).

Figure 9e,f show both the representative ECG and PPG (RL) signals during the fourth set of flight parabolas with the corresponding encountered acceleration (Figure 9c,d). Ten to fifteen seconds of ECG and PPGs sensor data were input from each micro and hypergravity parabolas and before each parabola set (e.g., pre-parabola, during 1 g) into our peak-finding algorithms to calculate a series of PAT and BPM data for both RL and LL that correspond to PAT from the leg with and without compression, respectively. The data were cut from their full-length to reduce physiological adaptation noise caused by gravity transitions. On average, the algorithm collected 12 peaks (standard deviation, SD = 2) for each hyper and microgravity segment. The mean PATs with their SD from all of these peaks during each hyper and microgravity period and for both the third and fourth parabola sets were then calculated and averaged.

The results of physiological sensor data processing for both the third and fourth parabola sets are depicted in Figure 10. As can be seen in both parabola sets, micro and hypergravity induced an increase in PAT from the pre-parabola state for both cases of RL and LL. In microgravity, there is a shift in fluid distribution from the lower to the upper body, where it is harder for the heart to pump blood toward the legs, resulting in decreased blood flow around these regions<sup>18</sup>. This corresponds to lower blood pressure and an increase in PAT, as reflected in Figure 10a,b. An increase can also be observed in the case of hypergravity, which can be explained by the high-angle and high-speed pull-up or "nose-up" maneuver of the parabola. As the subject lay down on the surface of the plane with the leg facing toward the nose most of the time, acceleration of the plane caused blood to pool toward the head, which reduced blood distribution around the leg. This led to an increase in PAT that was mostly higher than in the microgravity cases (except in LL, Set 3).

A trend can also be observed from the comparison between RL and LL. The leg with compression (RL) generally shows a higher PAT than the one without compression (LL) in both parabola sets. Previous studies concluded that external mechanical compression decreases regional arterial stiffness and PWV, and elicits significant vasodilation<sup>61,62</sup>. Since PWV is inversely proportional to PAT, our results thus agree with this study. However, there is no comparison data available of PAT from the same leg before and after compression due to the short duration of both micro and hypergravity periods. In this case, there is a possibility of anatomical difference between arteries of the subject's legs, which would introduce an offset to the PAT<sup>63</sup>.

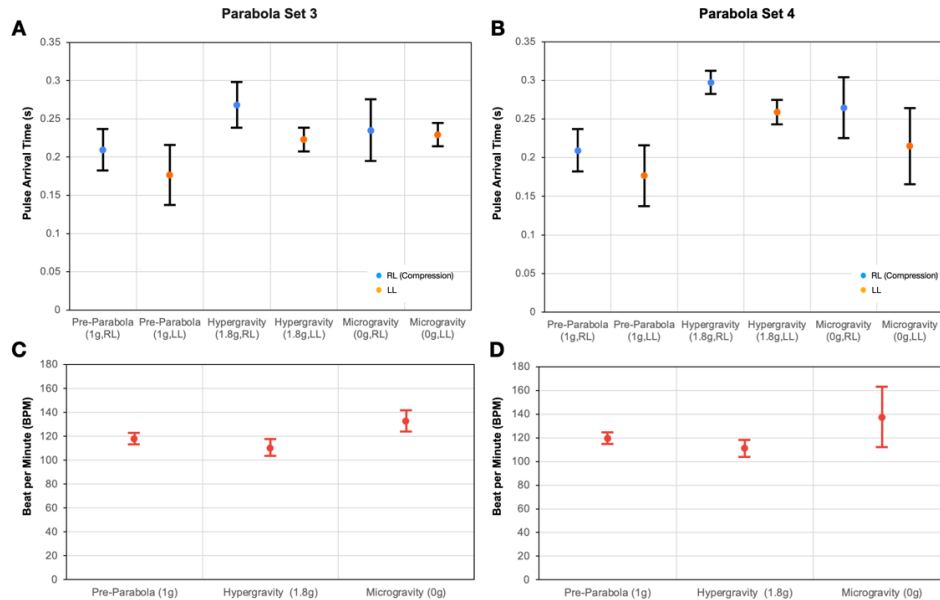


**Fig.10: Pulse arrival time between both legs of the subject (RL: compression, LL: without compression) during pre-parabola, hypergravity, and microgravity periods on the a) third and b) fourth set. c-d) Heart-rate in beats per minute (BPM) of the subject during pre-parabola, hypergravity, and microgravity periods on the third and fourth set, respectively (graph points and spreads correspond to the mean and SD).**

HR/BPMs are generally observed to be lower in microgravity due to the lack of gravitational pull on the body, which makes it easier for blood to return to the heart and reduces the workload on the cardiovascular system<sup>24</sup>. However, the BPM results between pre-parabola, hypergravity, and microgravity on both parabola sets show the opposite. There are other factors that could influence the heart rate, including the preceding hypergravity phases, as well as the mental stress and arousal of the subject<sup>21</sup>. Novice flyers, particularly those who have not experienced weightlessness, may experience an increase in heart rate during the parabolic flight due to excitement or anxiety<sup>64</sup>. The floating experience and sense of losing control and balance in microgravity periods triggers the release of adrenaline and other stress hormones that can cause sympathetic response through an increase in heart rate, while the activity of laying down during hypergravity periods could induce a sense of calmness, and through parasympathetic modulation, reduce heart-rate activity, as shown in our BPM data (Figure 10c,d). While these results demonstrate the functionality of our PS-Suit, further developments, experiments, and studies are still required. The short duration of parabolic flights only allow us to observe and analyze transient behaviors of physiological response as they hinder the cardiovascular system from reaching a steady state.

### C. Limitations and Future Work

This paper presents a design framework and a proof-of-principle validation of PS-Suit. However, there are limitations to the current design, which can be addressed through future developments and evaluations. One important consideration is the need for closed-loop feedback and control mechanisms to regulate the amount of compression in the suit based on input from fabric compression sensors and cardiovascular health parameters. It requires an intimate link and synchronization between the pneumatic and physiological and physical sensing systems. This effort will allow for a more controlled compression and effective intervention. Additionally, there is a need to develop firmware that can automate and simulate peristaltic compression throughout the spacesuit, which can help to improve circulation and reduce muscle fatigue<sup>65</sup>.

The current spacesuit design also only includes five inflatable chambers running from the waist to the ankle of one of the legs. While this provides some degree of intervention, it is limited in its effectiveness due to the scale and spatial resolution of the chambers. In order to address this limitation, future versions will need to include higher compression that covers a larger portion of the body, allowing for greater control over the level and timing of compression. This will require the development of modular pneumatic system hardware with air source and output extension, so it can accommodate the high number of miniature air chambers that are seamlessly embedded in the fabric of the suit. In

order to improve the wearability, breathability, and comfortability of spacesuits, combination of durable Nomex and TPU fibers and fabrics can be explored. By using digital fabrication tools and knitting these fibers into a custom full-body 3D garment based on a 3D body scan, one can develop a seamless PS-Suit that conforms to the unique shape of each individual astronaut. The knit and channel structures in the PS-Suit can also leverage multi-layer and computational design to maximize positive compression toward the body while optimizing mobility<sup>66</sup>. They could also be designed to provide axial load and pressure around the suit to help in mitigating musculoskeletal problems and spinal elongation relating to long-term microgravity exposures<sup>38</sup>.

Future evaluations should incorporate parabolic flight test on multiple subjects, including expert flyers who would exhibit more stable affective response, to evaluate how active compression of the PS-Suit can influence cardiovascular and other health parameters, including HR, RR, PAT, PWV, and BP. Through spatial compression and sensing, it is also possible to perform distributed oscillometry to measure blood pressure in primary locations of the human body. It would also be beneficial to test how the suit can function similarly to a LBNP chamber by providing an inverse pressure gradient to distribute blood flow toward the lower body during cruising and operation in long-term spaceflight. It can also simulate GCG, that aims to reduce OI during re-entry, landing, and post-landing by compressing the lower-body to shift blood distribution toward the upper body. Due to the short duration of zero-gravity in parabolic flights, ground testing through bed rest studies (exploiting different angles from head-down-tilt to upright bed rest) can also be leveraged to simulate some effects of weightlessness and monitor the transient and steady-state physiological change of the subject with and without active compression<sup>67</sup>. Ultimately, an ideal case will be evaluating PS-Suit functionality during a long-term space mission, as the astronauts launch from the Earth to the ISS, perform their daily tasks and experiments during IVA, and return to the Earth.

The PS-Suit platform could not only support cardiovascular health monitoring and microgravity adaptation, but also augment astronauts' physical training through active muscle compression, and provide emotional support and telepresence communication through comforting haptic transfer<sup>68</sup>. The design and control framework of the suit will also be applicable in other health, rehabilitation, exercise, or soft robotics applications, not only in outer space, but also on the Earth, in the form of anti-gravity suits, athletic or lymphedema compression garments, shapewear, corsets for exoskeleton and posture correction, and surgical tourniquets.

## VI. Conclusion

The PS-Suit is an active sensing-compression intravehicular activity spacesuit that can simultaneously perform wireless remote health diagnostics, as well as exert spatiotemporal pressure across the body. The suit has been designed to optimize wearability, functionality, and durability for each individual wearer. By integrating both physiological sensing and pneumatic actuation systems, the PS-Suit can facilitate closed-loop and timely response for astronauts to regulate their cardiovascular dynamics. Preliminary characterization and parabolic flight tests show the capabilities of the PS-Suit as a tool for researchers to correspondingly study the direct influence of active-dynamic compression and micro-to-hypergravity on various physiological markers. Overall, the PS-Suit has potential applications to safeguard the health of astronauts, and eventually civilian space travelers during their time in the ISS and extended voyages to the moon, Mars, and perhaps beyond.

## Acknowledgments

We would like to thank Ariel Ekblaw, Sean Auffinger, and Maggie Coblentz for their help in the planning, realization, and testing phase of this project, Shreyam Kacker for providing the parabolic flight IMU data, and Jeff Hoffman, Cady Coleman, Tony Antonelli, Nicholas de Monchaux, Juliana Cherston, Steve Boxall, ZERO-G Corporation, and the Responsive Environments Group. This work was funded through MIT Media Lab's Space Exploration Initiative NASA-TRISH Grant and the MIT Media Lab Research Consortia.

## References

- <sup>1</sup>Clément, G. *Fundamentals of Space Medicine*. Springer Science & Business Media, 2011.
- <sup>2</sup>Landon, L. B., Rokholt, C., Slack, K. J., and Pecena, Y. "Selecting Astronauts for Long-Duration Exploration Missions: Considerations for Team Performance and Functioning." *Reach*, Vol. 5, 2017, pp. 33–56.
- <sup>3</sup>Fortescue, P., Swinerd, G., and Stark, J. *Spacecraft Systems Engineering*. John Wiley & Sons, 2011.
- <sup>4</sup>Hill, T. R., and Johnson, B. J. EVA Space Suit Architecture: Low Earth Orbit vs. Moon vs. Mars. 2010.
- <sup>5</sup>Baker, E. S., Barratt, M. R., Sams, C. F., and Wear, M. L. Human Response to Space Flight. In *Principles of clinical medicine for space flight*, Springer, 2019, pp. 367–411.

- <sup>6</sup>Scheuring, R. A., Jones, J. A., Novak, J. D., Polk, J. D., Gillis, D. B., Schmid, J., Duncan, J. M., and Davis, J. R. "The Apollo Medical Operations Project: Recommendations to Improve Crew Health and Performance for Future Exploration Missions and Lunar Surface Operations." *Acta Astronautica*, Vol. 63, Nos. 7–10, 2008, pp. 980–987.
- <sup>7</sup>Johnson, R. L., Hoffer, G. W., Nicogossian, A. E., Bergman, S. A., and Jackson, M. M. "Lower Body Negative Pressure: Third Manned Skylab Mission." *Biomedical results from Skylab*, Vol. 377, 1977, p. 284.
- <sup>8</sup>Marshall-Goebel, K., Laurie, S. S., Alferova, I. V., Arbeille, P., Auñón-Chancellor, S. M., Ebert, D. J., Lee, S. M. C., Macias, B. R., Martin, D. S., and Pattarini, J. M. "Assessment of Jugular Venous Blood Flow Stasis and Thrombosis during Spaceflight." *JAMA network open*, Vol. 2, No. 11, 2019, pp. e1915011–e1915011.
- <sup>9</sup>Carvil, P., Baptista, R., and Russomano, T. "The Human Body in a Microgravity Environment: Long Term Adaptations and Countermeasures." *Aviation in Focus-Journal of Aeronautical Sciences*, Vol. 4, No. 1, 2013, pp. 10–22.
- <sup>10</sup>Scott, J. P. R., Weber, T., and Green, D. A. "Introduction to the Frontiers Research Topic: Optimization of Exercise Countermeasures for Human Space Flight—Lessons from Terrestrial Physiology and Operational Considerations." *Frontiers in physiology*, Vol. 10, 2019, p. 173.
- <sup>11</sup>Griffin, B. N., Rashford, R., Gaylin, S., Bell, D., and Harro, J. The Wait-Less EVA Solution: Single-Person Spacecraft. In *ASCEND 2020*, 2020, p. 4170.
- <sup>12</sup>Platts, S. H., Tuxhorn, J. A., Ribeiro, L. C., Stenger, M. B., Lee, S., and Meck, J. V. "Compression Garments as Countermeasures to Orthostatic Intolerance." *Aviation, space, and environmental medicine*, Vol. 80, No. 5, 2009, pp. 437–442.
- <sup>13</sup>Waldie, J. M., and Newman, D. J. "A Gravity Loading Countermeasure Skinsuit." *Acta Astronautica*, Vol. 68, Nos. 7–8, 2011, pp. 722–730.
- <sup>14</sup>Artiles, A. D., Trigg, C., Jethani, H., Tritchler, S., and Newman, D. Physiological and Comfort Assessment of the Gravity Loading Countermeasure Skinsuit during Exercise. 2016.
- <sup>15</sup>Granberry, R., Dunne, L., and Holschuh, B. Effects of Anthropometric Variability and Dimensional Change Due to Posture on Orthostatic Intolerance Garments. 2017.
- <sup>16</sup>Wicaksono, I., Shtarbanov, A., Slater, R., Ranade, E., and Paradiso, J. Peristaltic (PS) Suit: Active Bioelectronic Sensing-Compression Spacesuit for Microgravity Adaptation and Cardiovascular Deconditioning. In *ASCEND 2022*, 2022, p. 4208.
- <sup>17</sup>Zhu, M., Do, T. N., Hawkes, E., and Visell, Y. "Fluidic Fabric Muscle Sheets for Wearable and Soft Robotics." *Soft robotics*, Vol. 7, No. 2, 2020, pp. 179–197.
- <sup>18</sup>Hargens, A. R., and Richardson, S. "Cardiovascular Adaptations, Fluid Shifts, and Countermeasures Related to Space Flight." *Respiratory physiology & neurobiology*, Vol. 169, 2009, pp. S30–S33.
- <sup>19</sup>Heer, M., and Paloski, W. H. "Space Motion Sickness: Incidence, Etiology, and Countermeasures." *Autonomic Neuroscience*, Vol. 129, Nos. 1–2, 2006, pp. 77–79.
- <sup>20</sup>Lee, S. M. C., Ribeiro, L. C., Laurie, S. S., Feiveson, A. H., Kitov, V. V., Kofman, I. S., Macias, B. R., Rosenberg, M., Rukavishnikov, I. V., and Tomilovskaya, E. S. "Efficacy of Gradient Compression Garments in the Hours after Long-Duration Spaceflight." *Frontiers in physiology*, Vol. 11, 2020, p. 784.
- <sup>21</sup>Aerts, W., Joosen, P., Widjaja, D., Varon, C., Vandeput, S., Van Huffel, S., and Aubert, A. Heart Rate and Blood Pressure Variability under Moon, Mars and Zero Gravity Conditions during Parabolic Flights. No. 706, 2012, pp. 1.
- <sup>22</sup>McCall, C., Rostovsky, R., Wiard, R. M., Inan, O. T., Giovangrandi, L., Cuttino, C. M., and Kovacs, G. T. A. Noninvasive Pulse Transit Time Measurement for Arterial Stiffness Monitoring in Microgravity. 2015.
- <sup>23</sup>Wood, K. N., Greaves, D. K., and Hughson, R. L. "Interrelationships between Pulse Arrival Time and Arterial Blood Pressure during Postural Transitions before and after Spaceflight." *Journal of Applied Physiology*, Vol. 127, No. 4, 2019, pp. 1050–1057.
- <sup>24</sup>Baevsky, R. M., Baranov, V. M., Funtova, I. I., Diedrich, A., Pashenko, A. V., Chernikova, A. G., Drescher, J., Jordan, J., and Tank, J. "Autonomic Cardiovascular and Respiratory Control during Prolonged Spaceflights Aboard the International Space Station." *Journal of Applied Physiology*, Vol. 103, No. 1, 2007, pp. 156–161.
- <sup>25</sup>Hughson, R. L. Studying Cardiovascular Health in Microgravity. [https://blogs.nasa.gov/ISS\\_Science\\_Blog/2016/05/04/studying-cardiovascular-health-in-microgravity/](https://blogs.nasa.gov/ISS_Science_Blog/2016/05/04/studying-cardiovascular-health-in-microgravity/). Accessed Sep. 18, 2022.
- <sup>26</sup>Wicaksono, I., Tucker, C. I., Sun, T., Guerrero, C. A., Liu, C., Woo, W. M., Pence, E. J., and Dagdeviren, C. "A Tailored, Electronic Textile Conformable Suit for Large-Scale Spatiotemporal Physiological Sensing in Vivo." *npj Flexible Electronics*, 2020. <https://doi.org/10.1038/s41528-020-0068-y>.
- <sup>27</sup>Zhang, H., Li, W., Tao, X., Xu, P., and Liu, H. Textile-Structured Human Body Surface Biopotential Signal Acquisition Electrode. 2011.
- <sup>28</sup>Heo, J. S., Eom, J., Kim, Y. H., and Park, S. K. Recent Progress of Textile-Based Wearable Electronics: A Comprehensive Review of Materials, Devices, and Applications. *Small*.
- <sup>29</sup>Payra, S., Wicaksono, I., Cherston, J., Honnet, C., Sumini, V., and Paradiso, J. A. "Feeling Through Spacesuits: Application of Space-Resilient E-Textiles to Enable Haptic Feedback on Pressurized Extravehicular Suits." In *2021 IEEE Aerospace Conference (SO100)*, pp. 1–12. 2021.
- <sup>30</sup>Wicaksono, I., Cherston, J., and Paradiso, J. A. "Electronic Textile Gaia: Ubiquitous Computational Substrates Across Geometric Scales." *IEEE Pervasive Computing*, 2021.
- <sup>31</sup>Cherston, J., and Paradiso, J. A. "SpaceSkin: Development of Aerospace-Grade Electronic Textile for Simultaneous Protection and High Velocity Impact Characterization." *Sensors and Smart Structures Technologies for Civil, Mechanical, and Aerospace Systems*, 2019. <https://doi.org/10.1117/12.2513962>.



- <sup>32</sup>Villa-Colín, J., Shaw, T., Toscano, W., and Cowings, P. Evaluation of Astroskin Bio-Monitor during High Intensity Physical Activities. No. 5, 2018, pp. 262–265.
- <sup>33</sup>Dalsgaard, C., and Sterrett, R. “White Paper on Smart Textile Garments and Devices: A Market Overview of Smart Textile Wearable Technologies.” *Market Opportunities for Smart Textiles, Ohmatex, Denmark*, 2014.
- <sup>34</sup>Tasnim, F., Sadraei, A., Datta, B., Khan, M., Choi, K. Y., Sahasrabudhe, A., Vega Gálvez, T. A., Wicaksono, I., Rosello, O., Nunez-Lopez, C., and Dagdeviren, C. Towards Personalized Medicine: The Evolution of Imperceptible Health-Care Technologies. *Foresight*, 2018.
- <sup>35</sup>Bellisle, R., Bjune, C., and Newman, D. “Considerations for Wearable Sensors to Monitor Physical Performance during Spaceflight Intravehicular Activities.” In *2020 42nd Annual International Conference of the IEEE Engineering in Medicine & Biology Society (EMBC)*, pp. 4160-4164. 2020.
- <sup>36</sup>Ekblaw, A., Cherston, J., Liu, F., Wicaksono, I., Haddad, D. D., Valentina, S., and Paradiso, J. A. “From UbiComp to Universe—Moving Pervasive Computing Research Into Space Applications.” *IEEE Pervasive Computing*, 2023.
- <sup>37</sup>Petersen, N., Jaekel, P., Rosenberger, A., Weber, T., Scott, J., Castrucci, F., Lambrecht, G., Ploutz-Snyder, L., Damann, V., and Kozlovskaya, I. “Exercise in Space: The European Space Agency Approach to in-Flight Exercise Countermeasures for Long-Duration Missions on ISS.” *Extreme physiology & medicine*, Vol. 5, No. 1, 2016, pp. 1–13.
- <sup>38</sup>Bellisle, R., Ortiz, C., Porter, A., Harvey, A., Arquilla, K., Bjune, C., Waldie, J., and Newman, D. “The Mk-7 Gravity Loading Countermeasure Skinsuit: Evaluation and Preliminary Results.” In *2022 IEEE Aerospace Conference (AERO)*, pp. 1-11. 2022.
- <sup>39</sup>Jacobs, S., and Doherty, M. Prevention of Orthostatic Intolerance for Post-Shuttle Operations: A Comparison of Active and Passive Garments. 2011.
- <sup>40</sup>Stenger, M. B., Brown, A. K., Lee, S., Locke, J. P., and Platts, S. H. “Gradient Compression Garments as a Countermeasure to Post-Spaceflight Orthostatic Intolerance.” *Aviation, space, and environmental medicine*, Vol. 81, No. 9, 2010, pp. 883–887.
- <sup>41</sup>Stenger, M. B., Lee, S., Westby, C. M., Ribeiro, L. C., Phillips, T. R., Martin, D. S., and Platts, S. H. “Abdomen-High Elastic Gradient Compression Garments during Post-Spaceflight Stand Tests.” *Aviation, Space, and Environmental Medicine*, Vol. 84, No. 5, 2013, pp. 459–466.
- <sup>42</sup>Holschuh, B. T., and Newman, D. J. “Morphing Compression Garments for Space Medicine and Extravehicular Activity Using Active Materials.” *Aerospace medicine and human performance*, Vol. 87, No. 2, 2016, pp. 84–92.
- <sup>43</sup>Duvall, J., Granberry, R., Dunne, L. E., Holschuh, B., Johnson, C., Kelly, K., Johnson, B., and Joyner, M. The Design and Development of Active Compression Garments for Orthostatic Intolerance. No. 40672, 2017, pp. V001T01A013.
- <sup>44</sup>Newman, D., Hoffman, J., Bethke, K., Blaya, J., Carr, C., and Pitts, B. “Astronaut Bio-Suit System for Exploration Class Missions.” *NIAC Phase II Final Report*, 2005.
- <sup>45</sup>NASA. Rubber Vacuum Pants That Suck. [https://blogs.nasa.gov/ISS\\_Science\\_Blog/2015/06/02/rubber-vacuum-pants-that-suck/](https://blogs.nasa.gov/ISS_Science_Blog/2015/06/02/rubber-vacuum-pants-that-suck/). Accessed May 1, 2023.
- <sup>46</sup>Attias, J., Philip, A. T. C., Waldie, J., Russomano, T., Simon, N. E., and David, A. G. “The Gravity-Loading Countermeasure Skinsuit (GLCS) and Its Effect upon Aerobic Exercise Performance.” *Acta Astronautica*, Vol. 132, 2017.
- <sup>47</sup>NASA. Launch Entry Suit. [https://commons.wikimedia.org/wiki/File:Launch\\_entry\\_suit.jpg](https://commons.wikimedia.org/wiki/File:Launch_entry_suit.jpg). Accessed May 1, 2023.
- <sup>48</sup>Space, C. New Exhibit Tells “stranger than Fiction” Tale of Aerospace Medicine. <http://www.collectspace.com/news/news-070221a-stranger-than-fiction-aerospace-medicine-museum-of-flight.html>. Accessed May 1, 2023.
- <sup>49</sup>Wicaksono, I., and Paradiso, J. A. “FabricKeyboard : Multimodal Textile Sensate Media as an Expressive and Deformable Musical Interface.” *Proceedings of the International Conference on New Interfaces for Musical Expression*, 2017.
- <sup>50</sup>Wicaksono, I., Hwang, P. G., Droubi, S., Wu, F. X., Serio, A. N., Yan, W., and Paradiso, J. A. “3DKnITS: Three-Dimensional Digital Knitting of Intelligent Textile Sensor for Activity Recognition and Biomechanical Monitoring.” In *44th Annual International Conference of the IEEE Engineering in Medicine & Biology Society (EMBC)*, pp. 2403-2409. 2022.
- <sup>51</sup>Shtarbanov, A. “FlowIO Development Platform--The Pneumatic “Raspberry Pi” for Soft Robotics.” In *Extended abstracts of the 2021 CHI conference on human factors in computing systems*, pp. 1-6. 2021.
- <sup>52</sup>Karlsson, A., Rosander, J., Romu, T., Tallberg, J., Grönqvist, A., Borga, M., and Dahlqvist Leinhard, O. “Automatic and Quantitative Assessment of Regional Muscle Volume by Multi-atlas Segmentation Using Whole-body Water–Fat MRI.” *Journal of Magnetic Resonance Imaging*, Vol. 41, No. 6, 2015, pp. 1558–1569.
- <sup>53</sup>Risso, A., Ciana, A., Achilli, C., Antonutto, G., and Minetti, G. “Neocytolysis: None, One or Many? A Reappraisal and Future Perspectives.” *Frontiers in physiology*, Vol. 5, 2014, p. 54.
- <sup>54</sup>Zeagler, C. Where to Wear It: Functional, Technical, and Social Considerations in on-Body Location for Wearable Technology 20 Years of Designing for Wearability. 2017.
- <sup>55</sup>Liu, R., Lao, T. T., Little, T. J., Wu, X., and Ke, X. “Can Heterogeneous Compression Textile Design Reshape Skin Pressures? A Fundamental Study.” *Textile Research Journal*, Vol. 88, No. 17, 2018, pp. 1915–1930.
- <sup>56</sup>Fratto, L. A., and others. “Evaluating the Performance of Fibers and Fabrics for Astronaut’s IVA Wardrobes for Long Duration Space Flight.” 2005.
- <sup>57</sup>Özlenen, E., and Paul, R. Composite Textiles in High-Performance Apparel. In *High-performance apparel*, Elsevier, 2018, pp. 377–420.
- <sup>58</sup>Zhou, B., Chen, X., Hu, X., Ren, R., Tan, X., Fang, Z., and Xia, S. A Bluetooth Low Energy Approach for Monitoring Electrocardiography and Respiration. 2013.
- <sup>59</sup>Bagha, S., and Shaw, L. “A Real Time Analysis of PPG Signal for Measurement of SpO2 and Pulse Rate.” *International journal of computer applications*, Vol. 36, No. 11, 2011, pp. 45–50.

<sup>60</sup>Block, R. C., Yavarimanesh, M., Natarajan, K., Carek, A., Mousavi, A., Chandrasekhar, A., Kim, C.-S., Zhu, J., Schifitto, G., Mestha, L. K., and others. "Conventional Pulse Transit Times as Markers of Blood Pressure Changes in Humans." *Scientific Reports*, Vol. 10, No. 1, 2020, p. 16373.

<sup>61</sup>Heffernan, K. S., Edwards, D. G., Rossow, L., Jae, S. Y., and Fernhall, B. "External Mechanical Compression Reduces Regional Arterial Stiffness." *European journal of applied physiology*, Vol. 101, 2007, pp. 735–741.

<sup>62</sup>Szolnoky, G., Gavallér, H., Gönczy, A., Bihari, I., Kemény, L., Forster, T., and Nemes, A. "The Effects of Below-Knee Medical Compression Stockings on Pulse Wave Velocity of Young Healthy Volunteers." *The Journal of Strength & Conditioning Research*, Vol. 35, No. 1, 2021, pp. 275–279.

<sup>63</sup>Sondej, T., Sieczkowski, K., Olszewski, R., and Dobrowolski, A. "Simultaneous Multi-Site Measurement System for the Assessment of Pulse Wave Delays." *Biocybernetics and Biomedical Engineering*, Vol. 39, No. 2, 2019, pp. 488–502.

<sup>64</sup>Johnson, K. T., Taylor, S., Fedor, S., Jaques, N., Chen, W., and Picard, R. W. *Vomit Comet Physiology: Autonomic Changes in Novice Flyers*. 2018.

<sup>65</sup>Zhu, M., Ferstera, A., Dinulescu, S., Kastor, N., Linnander, M., Hawkes, E. W., and Visell, Y. "A Peristaltic Soft, Wearable Robot for Compression and Massage Therapy." *arXiv preprint arXiv:2206.01339*, 2022.

<sup>66</sup>Tessmer, L., Goldstein, G., Herrera-Arcos, G., Korolovych, V., Bellisle, R., Paige, C., Shallal, C., Sahasrabudhe, A., Herr, H., Boriskina, S., Newman, D., and Tibbits, S. "3D Knit Spacesuit Sleeve with Multifunctional Fibers and Tunable Compression." In *ACADIA 2022*.

<sup>67</sup>Watenpaugh, D. E. "Analogues of Microgravity: Head-down Tilt and Water Immersion." *Journal of Applied Physiology*, Vol. 120, No. 8, 2016, pp. 904–914.

<sup>68</sup>Teh, J.K.S., Adrian, D. C., Roshan, L. P. Yongsoo, C., Vuong, T., and Sha, L. "Huggy Pajama: a mobile parent and child hugging communication system." In *Proceedings of the 7th international conference on Interaction design and children*, pp. 250-257. 2008.